Indian Journal of Radio & Space Physics
Vol 43, June 2014, pp 205-212

Modelling of the equatorial ionospheric E-layer based on cosχ index

A K Kazeem[1], J O Adeniyi[1] & A T Adediji[2,$,*]

[1]Department of Physics, University of Ilorin, P M B 1515, Ilorin, Nigeria
[2]Department of Physics, Federal University of Technology, P M B 704, Akure, Nigeria
[$]E-mail: kunleadediji2002@yahoo.co.uk; kadediji@futa.edu.ng

Received 28 May 2013; revised 17 February 2014; accepted 26 February 2014

Daytime hourly values of the critical frequency of the ionospheric E-layer, *f*oE, obtained at Ouagadougou Ionospheric Observatory (12.4°N, 1.5°W) in Burkina Faso, West Africa, an equatorial station, during the solar cycle 22 (1985 – 1995) have been used to develop a model based on solar zenith angle through cosχ index factor using the relation $f\text{oE} = a\,(\cos\chi)^n$. The average value of the diurnal cosχ index, n, at Ouagadougou was found to be 0.30 for both low and high solar activity. The model was tested with *f*oE data from Korhogo (9.3°N, 5.4°W) in Cote-d'Ivoire, another equatorial station, and there is good agreement between the model and observations. The validity of the *f*oE model was also compared with predicted values by IRI-2012 model and good agreement has been observed. The percentage difference, when *f*oE observed compared with IRI-2012 model, was found to be within ±10% for both equinoxes and solstices for the two levels of solar activity.

Keywords: Equatorial ionospheric model, Critical frequency, Diurnal cosχ index, Solar zenith angle, Ionospheric E-layer peak

PACS Nos: *94.20.dg; 94.20.dt*; 94.20.Cf; *96.60.qd*

1 Introduction

The ionospheric E-layer has been studied for many years and the main features are well described by simple Chapman theory[1]. The physics involved is, particularly, simple for the E-layer, where the ionization time constant is only a few minutes, so that conditions are always close to equilibrium. The ionospheric E-layer can provide relatively stable mode of propagation. So, it is of great importance to predict the E-region parameters, especially the critical frequency accurately and economically[2].

Modelling of the ionospheric parameters, such as electron density profiles, electron temperature, ion composition (O^+, H^+, N^+, He^+, O_2^+, NO^+, $Cluster^+$), ion temperature and ion drift over the whole altitude range for all geographic positions, time spans, and geophysical conditions are essential part of ionospheric physics and ionospheric space weather applications. A multitude of different ionospheric models, including theoretical, empirical and semi-empirical model, are available based on variety of international and national organization modeling programs. Many recent reviews have been published about ionospheric models. The most recent ones are proposed by Cander *et al.*[3] and Bilitza[4]. Empirical models, which are established by statistical analysis of measured data, are widely investigated since they have the advantage of representing the ionosphere through actual measurements[2]. Many local, regional and global empirical ionospheric models have been developed over the past years. The International Reference Ionosphere (IRI) is probably the most mature of these models, having undergone more than two decades of scrutiny and improvement. It is an empirical model based on a wide range of ground and space data. It gives monthly averages of the ionospheric parameters in the altitude range 50-1500 km in the non-auroral ionosphere[5]. IRI-2012 is the latest version of the model, which has been improved significantly and new parameters have been introduced[6]. This model has been used in the present study although this model did not have any modification on the electron density changes (or its equivalent critical frequency). It is, generally, believed that the normal E-layer follows the Chapman layer variation which satisfies the expression:

$$N_m E = N_O (\cos\chi)^{2p} \quad \ldots (1)$$

where, N_mE, is the maximum electron density of the layer; N_o, the normalized density; and χ, the solar zenith angle. Solar zenith angle, χ, also called the zenith distance, is the angle between the local zenith and the line joining the observer and the sun. It is an

angle between 0° and 90°. For the ideal Chapman layer, the index p is equal to 0.25. In practice, it is found that the value of p depends on whether diurnal or seasonal variations are being considered[7]. However, Lyon[8] observed that the exponent p at Ibadan, Nigeria shows no significant difference between seasonal variations and its diurnal value, which was reported to be 0.32. This was confirmed to be valid at 0800, 1200 and 1600 hrs LT for both sunspot maximum of 1957/1958 and minimum of 1964. The studies of normal E-layer have been concentrated on mid-latitude than equatorial normal E-layer. More precise information about the E-layer is, therefore, available for the mid-latitudes than for equatorial latitudes. For instance, diurnal cosχ index for each month of the year and the seasonal cosχ index for daylight hours (0700 - 1700 hrs LT) have been reported for many mid-latitude stations, e.g. Appleton & Lyon[9], Beynon & Brown[10], Hibberd & Henderson[11]. Such detailed study has not been reported for equatorial latitudes especially in African sector, although Adeniyi & Awe[12] worked on E-layer at equatorial latitude, but this is not sufficient. Studies of E-layer at equatorial ionospheric stations focused more on E-region irregularities and drift measurements rather than the normal E-layer[13]. The purpose of this paper is to develop a model of foE over Ouagadougou, Burkina Faso, an equatorial station, for prediction of an equatorial ionospheric E-layer using a long time series of ionosonde data.

There are many local and regional ionospheric models related to the E-layer critical frequency. Zolesi *et al.*[14] developed a regional ionospheric model by using Fourier analysis on monthly median values of local and regional ionospheric models related to the E-layer critical requency. Zolesi *et al.*[14] developed a regional ionospheric model by using Fourier analysis on monthly median values of ionospheric characteristics including foE from seven ionospheric stations in Europe. Holt & Zhang[15] constructed a detailed empirical model of ionospheric E- and F-region over Millstone Hill. Mickinnel & Poole[16] developed a model over Grahams town, South Africa, using neural networks. Yue *et al.*[2] constructed an empirical model of foE over Wuhan, China using long time series of ionosonde data.

2 Data and Method of analysis

The ionospheric foE data used in this study were obtained from Ouagadougou in Burkina Faso, an equatorial station (12.4°N, 1.5°W, dip 5.9°N). The period of study covered the solar cycle 22 (1985-1995). Solar parameter, R_z12, and magnetic index, k_p, were used as auxiliary data to define the level of solar activity and of geomagnetic perturbation, respectively. The period of study was grouped into two: (i) 1988 - 1993, years of high solar activity; and (ii) 1985-1987 and 1994-1995, years of low solar activity. The annual mean sunspot number for the years of high and low solar activity ranged 55-158 and 13-30, respectively. In this study, monthly median patterns of the data is adopted in order to avoid the interference resulted from occasional mistakes in daily observation and investigate the average behaviour of E-layer. Hourly values of monthly median foE, for each period of study, were obtained during the daytime (0700-1700 hrs LT) and logarithm hourly monthly median foE values were also determined for the months of the years being considered. This study employs the relation between foE and cosχ given as:

$$f_oE = a(\cos\chi)^n \quad \ldots (2)$$

where, n, is the diurnal cosχ index; χ, the solar zenith angle; and a, coefficient. However, the above equation is applicable only when solar zenith is not big. The cosχ and log (cosχ) values were determined at the middle of month for each of the month during the year between 0700 and 1700 hrs LT. As cosχ values at 0600 and 1800 hrs LT are not reliable and the extreme angles do not fit the equation, these values are not used in this study. To get precise estimation of constants, a and n, the data, whose median counts are less than 6, is excluded to ensure the quality (there are 11 data points between 0700 and 1700 hrs LT in monthly median patterns of hourly data for each month).

To determine the effect of solar activity on foE, the daily solar flux F10.7 is used to represent solar activity level and was downloaded from National Geophysical Data Center (NGDC) Satellite and Information Service website (http:// www.spirdr.ngdc.noaa.gov/spirdr). Figure 1 (a) displays yearly mean values of F10.7 during 1985-1995 and Fig. 1(b) shows yearly foE values of local noon time during 1985-1995. A high correlation can be observed between these two parameters by comparing Fig. 1(a) and Fig. 1(b). It is known that temperature increases rapidly with height in the daytime in the E–region. This brings an increase in

the scale height, H = kT/mg and decrease in production rate. Including this effect[7], Eq. (2) can be expressed as:

$$f_oE = a(\cos)^{0.25(1+g)}, \text{ (n = 0.25)} \quad \ldots (3)$$

where, g = dH/dh, is the scale height gradient.

In order to include the effect of solar activity on foE, Eq. (2) can be further expressed as:

$$f_oE = A(1+aF10.7)(\cos\chi)^n \quad \ldots (4)$$

where, n = 0.25, is obtained from theory; A and a, are constants; and F10.7, the twelve month mean solar radio flux.

Monthly values of coefficient, a and the diurnal cosχ index, n, obtained each year for a solar cycle were used to obtain yearly average values and shown in Fig. 2. Figure 3 shows the linear regression plot of yearly foE values against yearly F10.7 for the period 1985-1995. In order to eliminate the varying solar zenith angle and seasonal effect, the values of foE at the same hour were used. In this work, noon time is chosen when χ = 0. Adeniyi & Awe[12] found that correlation coefficients between $N_mE(f\text{oE})^2$ and sunspot number (R) or solar radio flux (F10.7) at Ibadan (equatorial region) is as high as 0.97 at noon. The correlation at 1800 and 0600 hrs LT were 0.07 and 0.48, respectively depending on the time of day.

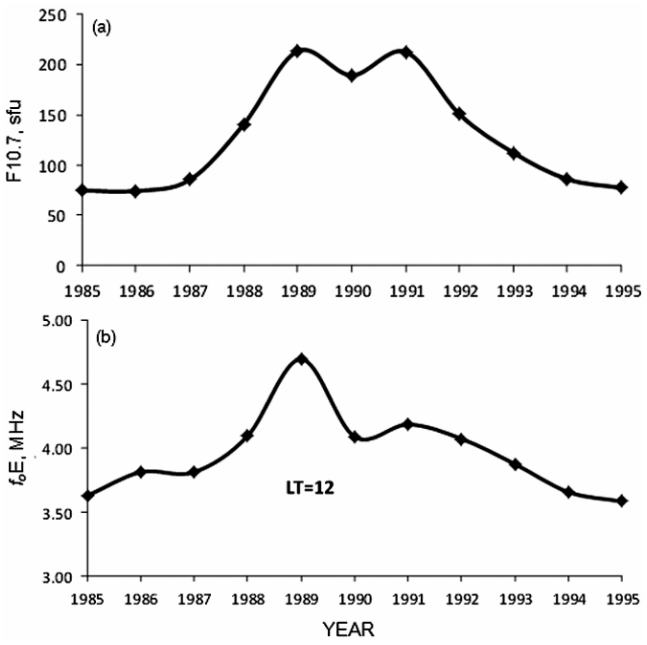

Fig. 1 — Yearly variation of: (a) solar radio flux (F10.7); and (b) critical frequency of E-layer (foE) of local noon time over a solar cycle (11 data points count each)

Also, to get precise value of the constants in Eq. (4), yearly values of both foE and F10.7 were adopted based on the fact that correlation studies between solar indices and ionospheric parameters is better for 12-month running mean and weaker for monthly and daily average[17]. To test the model, the year 1985 is selected to represent years of low solar activity and year 1991 is selected to represent years of high solar activity, The foE values were generated using Eq. (4):

$$f_oE = 3.3(1+0.0015F10.7)(\cos\chi)^{0.25} \quad \ldots (5)$$

The foE values were calculated for each hour on the 15th (middle day) of each month for the considered years. These hourly values are taken to be representative of the monthly hourly averages for the days of that month. These monthly averages were used to compute the seasonal averages. This was done for each of the year considered[2,18,19]. The geomagnetic field perturbations were avoided by assuming $k_p \leq 3$, which means quiet condition of the magnetosphere. Thus, the affected days were removed from monthly representation and not used in the seasonal averages. The hourly averages obtained in this way, were compared with the corresponding independent foE (observed data) obtained from Korhogo in Cote-d'Ivoire

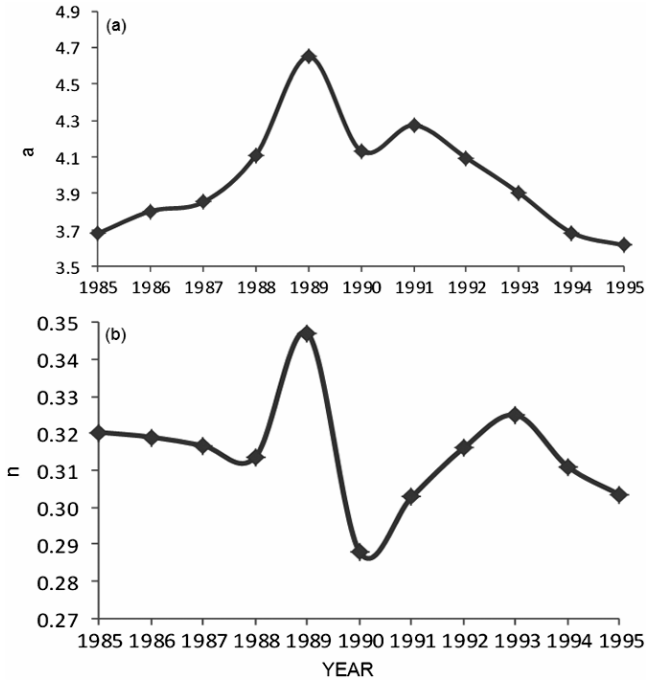

Fig. 2 — Yearly variation of: (a) coefficient a; and (b) the diurnal cos χ index n; over a solar cycle (1985-1995) (11 data points count each)

(9.3°N, 5.4°W, dip 0.67°S), an equatorial station. For the observed foE values, seasonal grouping was done by combining the hourly values of foE for all the days of the months of November, December and January (December solstice); February, March and April (March equinox); May, June and July (June solstice); August, September and October (September equinox)[18,20,21]. The model for the year 1985 with sunspot number (R_z12 = 18) was compared with data of 1995 with sunspot number (R_z12 = 18), also of year of low solar activity. The model for the year 1991 with sunspot number (R_z12 = 146) was compared with data of January to April 2000 with sunspot number (R_z12 = 120) and May to December 1999 with sunspot number (R_z12= 93) of period of high solar activity. It was not possible to get data of exactly the same year for both stations. But the years have been selected with comparable solar activities. Also, the data of January-April 1999 were not used because they were low. For further model validation, the model was compared with IRI, the IRI2012 model was used to generate foE IRI-2012 values for each 15th (middle day) of every month during the years 1985 and 1991. These hourly values are taken to be representatives of the monthly hourly means for the days of that month. These monthly averages were used to compute the seasonal averages[18,19]. The hourly (IRI) foE values were generated and downloaded from http://www.omniweb.gsfc.nasa.gov/vitmo/iri2012_vitmo.html. The hourly means obtained in this way were also compared with corresponding ones calculated using Eq. (5) (model). The percentage differences of the foE model from the foE observed and foE (IRI-2012) were also determined for each of the seasons of the considered years. This is necessary to test the validity of the present model. The standard deviations obtained from the observed values were used as error bars on the observed foE averages. This was done in order to determine if the differences between the model and observed foE were significant or not. The test was done to show whether the model portray the morphology of E-layer of equatorial ionosphere.

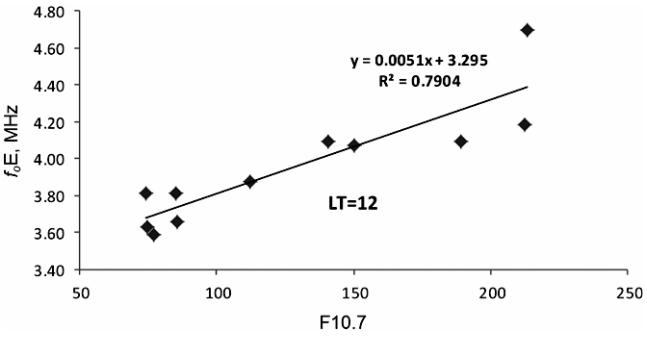

Fig. 3 — Regression plot of the yearly foE at noon time against yearly F10.7 over a solar cycle (1985–1995) (11 data points count)

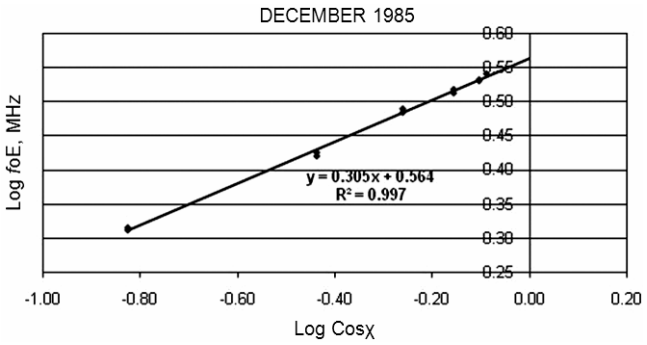

Fig. 4 — Plot of log foE against log cosχ for the year of low solar activity

3 Results and Discussion

3.1 Diurnal Cosχ

Figure 4 shows the typical example of the plot of log foE against log (cosχ) for each month of a period of low solar activity while Fig. 5 shows the typical example of the plot of log foE against log (cosχ) for each month for a period of high solar activity.

The average diurnal cosχ index (n) was evaluated during each month for years under consideration. The average diurnal cos χ index, n, for foE had the same value of 0.31 for both years of low and high solar activity at Ouagadougou and it does not depend on solar activity. This result agrees with results obtained by Lyon[8], Adeniyi & Awe[12], Kouris & Muggleton[22] and Araujo Pradere *et al.*[23].

The correlation coefficient (R) between the log (foE) and log (cosχ) is high, ranging 0.9391 - 0.9996 for low solar activity and 0.92 - 0.9995 for high solar activity. This indicates the existence of a relationship

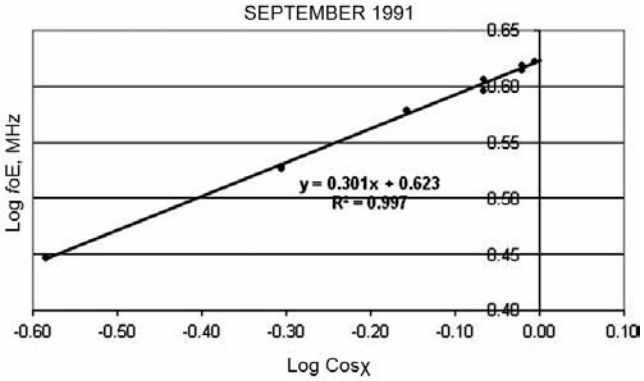

Fig. 5 — Plot of log foE against log cos χ for year of high solar activity (11 data points count each)

between the ionospheric parameter foE and solar zenith angle, χ. This suggests that foE may be represented by the relation $f\text{oE} = a\,(\cos\chi)^n$.

The result obtained in this work differs from 0.25, which is for ideal Chapman layer, the exponent p (or n) depends on the season and latitude. The p decreases with increase in latitude and gets closer to that of ideal Chapman layer outside the equatorial region and the departure is due to the influence of solar quiet (Sq) currents of E-layer. Also, differences between the actual average value of n ≈ 0.30, which is slightly larger than Chapman's theoretical value (n =0.25), may be explained by the existence of positive gradient of the scale height H (Ref. 7). This difference modifies the exponent of Eq. (2) by a factor (1+ g), where g = dH/dh = 0.2, in agreement with thermospheric models. Thus, changes in the recombination coefficient (∝) with height may be taken into account. In order to develop the present model, n = 0.25 is used as an index for Chapman layer if isothermal assumption is assumed and constant scale height dH/dh = 0.2 is eliminated.

3.2 Relationship between foE and solar activity

As can be seen in Fig. 2, 'a' has an obvious solar cycle variation, while 'n' does not. Figure 3 shows the linear regression of yearly foE value at noon time against yearly F10.7 during 1985 -1995. The values of constants a and A are 0.0015 and ≈ 3.3, respectively. These values are substituted to get Eq. (5), an empirical model over Ouagadougou. The regression coefficient is R^2 = 0.7904 and correlation coefficient is R= 0.8890. This strong positive correlation between foE and F10.7 shows the dependent of foE on solar activity.

3.3 Comparison of model with observations and IRI-2012 model

The diurnal variation of the foE (calculated ones) model, the observed and the IRI (2012) model for all the seasons at low and high solar activity are shown in Figs 6 and 7. The vertical lines are the standard deviations used as error bars centered on the mean values. It can be seen that the model, the observed values and the IRI-2012 model follow the same pattern, with foE rising from sunrise (0700 hrs LT) very sharply and get to a peak around noon (1200 hrs LT). A sharp decrease occurs after midday till sunset when foE attains minimum value around 1700 hrs LT. Very small deviation exist between the model and the observed values and the model and the IRI-2012 model. Departures were seen between the model and observed values, and also between the observed and

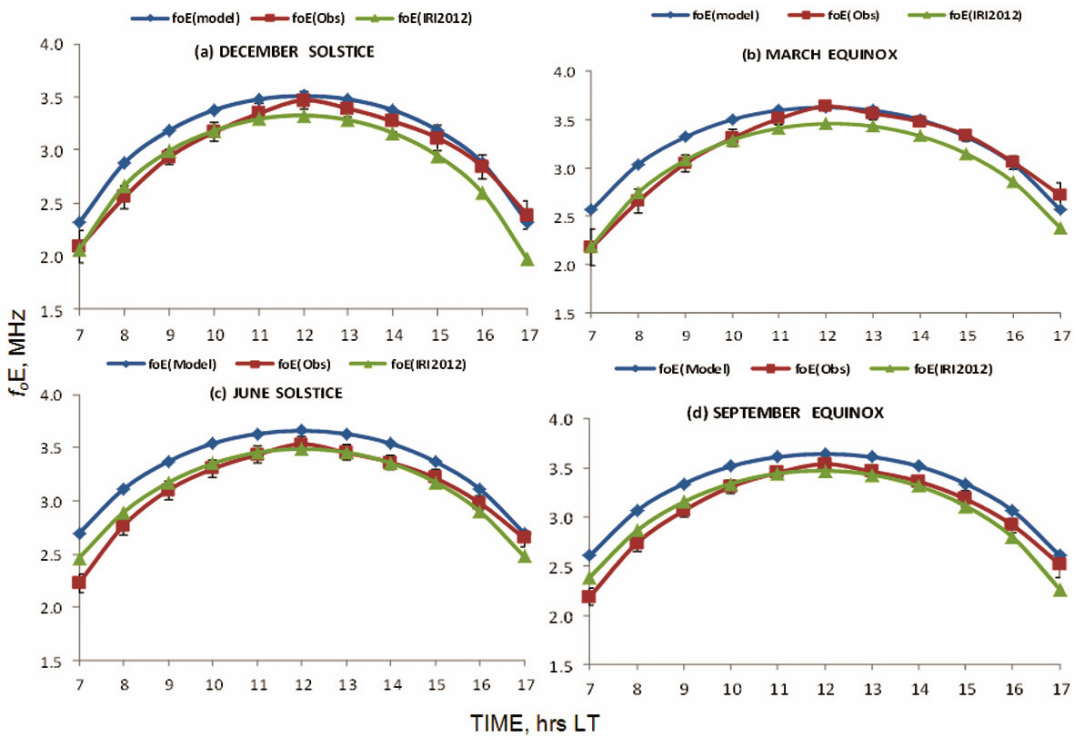

Fig. 6 — Diurnal variation of the model (1985), the observed foE (1995) and the IRI-2012 model (1985) at low solar activity during: (a) December solstice; (b) March equinox; (c) June solstice; and (d) September equinox (vertical lines are standard deviation used as error bars) (11 data points count each)

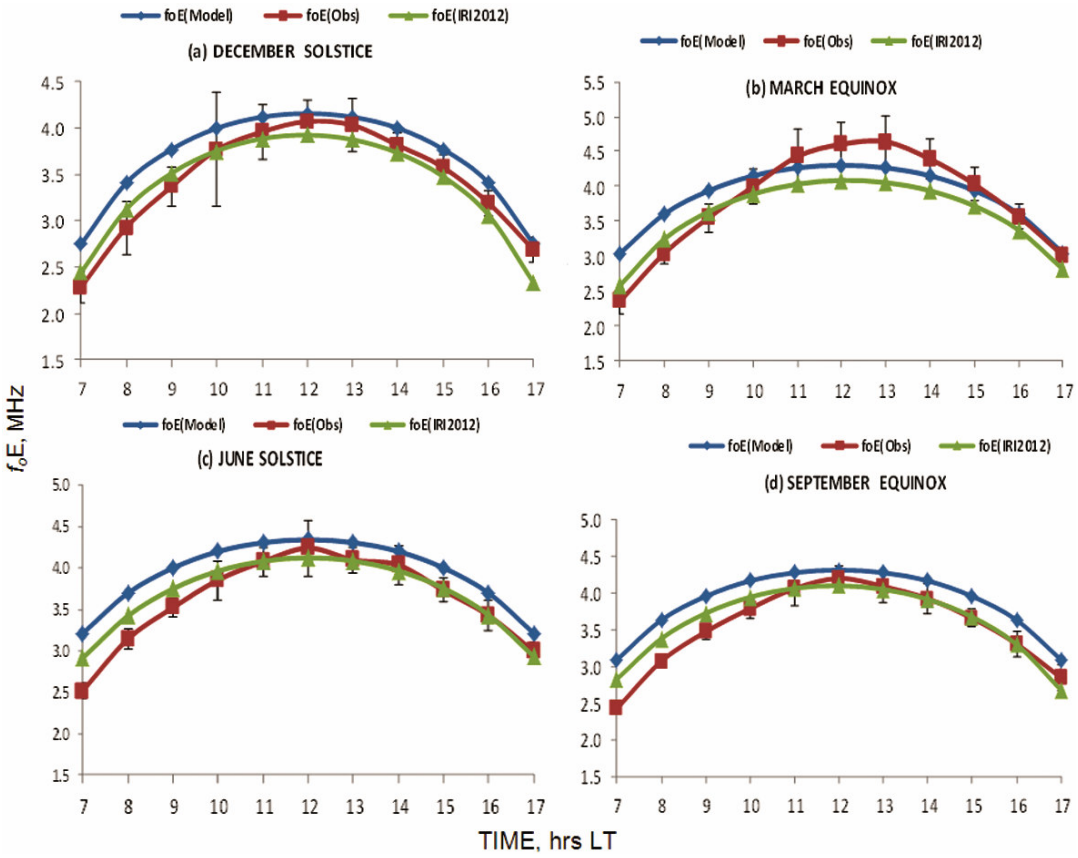

Fig. 7 — Diurnal variation of the model (1991), the observed *f*oE (1999/2000) and the IRI-2012 model (1991) at high solar activity during: (a) December solstice; (b) March equinox; (c) June solstice; and (d) September equinox (vertical lines are standard deviation used as error bars) (11 data points count each)

Table 1 — Hourly percentage differences in *f*oE between the model (1985) and the observed values in 1995, the year of low solar activity

Time, hrs LT	Seasons			
	December solstice	March equinox	June solstice	September equinox
0700	11	16	19	17
0800	12	13	12	11
0900	8	9	8	9
1000	6	6	7	6
1100	4	2	6	5
1200	1	0	4	3
1300	3	1	5	4
1400	3	1	5	6
1500	2	-1	5	5
1600	1	-1	4	5
1700	-2	-6	2	3

the IRI-2012 model around midday in March equinox during the year of high solar activity [Fig. 7(b)], observed *f*oE did not reach peak at 1200 hrs LT as expected but maximum value occurred at 1300 hrs LT, although deviations occur at any other time, but is very small. In order to look into the model in detail, the percentage differences between *f*oE (the model and observed values) and the model and IRI-2012 model were determined and deductions were made that validate the acceptability of our model.

Tables 1 and 2 show the hourly percentage differences in *f*oE, between the model and the observed values for low and high solar activity, respectively. The percentage differences in *f*oE are less than 10% for most of the time, except in the early hour (0700 and 0800 hrs LT) for all seasons at low solar activity; (0700 and 0800 hrs LT) in March equinox and (0700 and 0900 hrs LT) in other seasons at high solar activity, respectively.

Tables 3 and 4 show the hourly percentage differences in *f*oE, between the present model and the IRI-2012 model for low and high solar activity, respectively. The percentage differences in *f*oE are also less than 10% for most of the time for all seasons, except in the early and late hours (0700 and

Table 2 — Hourly percentage differences in foE between the model (1991) and observed values in 1999/2000, the year of high solar activity

Time, hrs LT	Seasons			
	December solstice	March equinox	June solstice	September equinox
0700	18	26	24	24
0800	15	17	16	17
0900	11	10	13	13
1000	6	4	9	9
1100	4	-4	5	5
1200	2	-7	2	3
1300	2	-8	5	5
1400	5	-6	4	6
1500	5	-2	7	9
1600	7	1	8	8
1700	2	1	7	8

Table 3 — Hourly percentage differences in foE between the model (1985) and the IRI-2012 model in 1985, the year of low solar activity

Time, hrs LT	Seasons			
	December solstice	March equinox	June solstice	September equinox
0700	11	16	9	9
0800	8	10	7	7
0900	6	7	6	6
1000	6	6	5	5
1100	5	5	5	5
1200	5	5	5	5
1300	6	5	5	5
1400	7	5	5	6
1500	8	5	6	7
1600	10	6	7	9
1700	16	7	9	14

1700 hrs LT) in December solstice, (0700 hrs LT) in March equinox, and (1700 hrs LT) in September equinox at low solar activity; (0700, 1600 and 1700 hrs LT) in December solstice, (0700 hrs LT) in March equinox, and (1700 hrs LT) in September equinox at high solar activity, respectively. Generally, the percentage differences between foE, the model and observed values, the model and IRI-2012 model are within ±10 for most of the time for all seasons of the years considered. The percentage differences in foE, between the model and the observations, the model and the IRI-2012 model for both solstices and equinoxes are quite small for the two levels of solar activity.

Studies on the general morphology of the equatorial ionosphere have shown that it is characterized by a single peak, which occurs around noon. The present model confirms this feature of foE of equatorial region, which occurs as a result of intensity of radiation from the sun which increases from sunrise and attains peak around midday when $\chi = 0$ and the intensity of solar radiation decreases afterwards till night when the underlying ionization is negligible.

Table 4 — Hourly percentage differences in foE between the model (1991) and the IRI-2012 model in 1991, the year of high solar activity

Time, hrs LT	Seasons			
	December solstice	March equinox	June solstice	September equinox
0700	12	16	10	9
0800	9	10	8	7
0900	7	8	6	6
1000	6	7	6	5
1100	6	6	5	5
1200	6	5	5	5
1300	6	5	5	5
1400	7	5	6	6
1500	8	6	6	7
1600	11	7	7	10
1700	16	8	9	14

The model, observations and IRI-2012 model follow the same trend, very good agreement exist between them except around midday in March equinox at high solar activity [Fig. 7(b)]. The observed foE, deviated from the model and also from the IRI-2012 model, it may be due to ionospheric disturbances but the differences are not significant. The model was tested and found to predict fairly accurately for the equatorial region.

4 Conclusions

About 11 years worth of data from the ionosonde station in Ouagadougou, Burkina Faso (dip = 5.9) were used to develop a model for prediction of equatorial E-layer. The average value of the diurnal cosχ or Chapman index (n) found through linear regression matches closely Chapman's predictions with a high correlation coefficient if the isothermal assumption is eliminated and constant gradient of scale height dH/dh = 0.2, are assumed. The data for two years was used to test the model: (i) year 1985 to represent the years of low solar activity and (ii) year 1991 to represent the years of high solar activity. The model was tested with foE data from Korhogo, Cote-d'Ivoire (dip 0.67) and also tested with IRI model. There is good agreement between the developed model and observations, and

developed model and IRI model. The percentage differences between foE, the developed model and observed values and the developed model and IRI-2012 model for most of the time were found to be within ±10 for both solstices and equinoxes, which are quite small for the two levels of solar activity. The developed model was found to be fairly accurate for the prediction of E-layer of the equatorial ionosphere. However, there is need to conduct similar investigations for other latitudinal regions.

Acknowledgement

The authors are grateful to the host of the ionosonde equipments in Ouagadougou and Korhogo for preserving and making the data available for this research work. The authors are also grateful to National Geophysical Data Center (NGDC) NOAA satellite and information service, the F10.7 indices are downloaded from the SPIDR website (http://spidr.ngdc.noaa.gov/spidr). They also like to appreciate NASA and NSSDC for making IRI-2012 model (online version) available for scientific use.

References

1 Titheridge J E, Modelling the peak of the ionospheric E-layer, *J Atmos Sol-Terr Phys (UK)*, 62 (2000) pp 93-114.

2 Yue X, Wan W, Liu L & Ning B, An empirical model of ionospheric *f*oE over Wuhan, *Earth, Planets Space (Japan)*, 58 (2006) pp 323-330.

3 Cander L R, Leitinger R & Levy M F, Ionospheric models including the auroral environment, in *Workshop on Space Weather Report WPP-155* (European Space Agency, Noordwijk, The Netherlands), 1999, pp 135-142.

4 Bilitza D, Ionospheric models for radio propagation studies, in *The Review of Radio Science 1999-2002*, edited by W R Stone (IEEE Press, Piscataway, NJ), 2002, pp 625-679.

5 Bilitza D & Reinisch B W, International Reference Ionosphere 2007: Improvements and new parameters, *Adv Space Res (UK)*, 42 (4) (2008) pp 599- 609.

6 Bilitza D & Mckinnell L A, International Reference Ionosphere- A tool for space weather applications: Recent developments, *Geophys Res Abs (Germany)*, 14 (2012) pp 12927.

7 Rishbeth H & Garriott O K, *Introduction to ionospheric physics* (Academic Press, New York), 1969.

8 Lyon A J, The E- layer at Ibadan, *Proceedings of the International Symposium on Equatorial Aeronomy I-A* (ISEA-3) (Physical Research Laboratory, Ahmedabad), 1969, pp 211.

9 Appleton E V & Lyon A J, Studies of E-layer of ionosphere II: Electromagnetic perturbations and other anomalies, *J Atmos Sol-Terr Phys (UK)*, 21 (1961) pp 73-99.

10 Beynon W J G & Brown G M, Geomagnetic distortion of region-E, *J Atmos Sol-Terr Phys (UK)*, 14 (1959) pp 138-166.

11 Hibberd F H & Henderson T L E, Sq current effects on the seasonal variations in the E region of the ionosphere, *J Atmos Sol-Terr Phys (UK)*, 29 (1967) pp 477– 488.

12 Adeniyi J O & Awe O, The regular ionospheric E-layer at Ibadan during daytime, *Proc Nigerian Acad Sci*, 1 (1984) pp 49-61.

13 Oyinloye J O & Onolaja G B, Solar cycle variation of ionospheric E- region horizontal drifts at Ibadan, *J Atmos Sol-Terr Phys (UK)*, 39 (11-12) (1977) pp 1353-1356.

14 Zolesi B, Cander L R & De Franceschi G, Simplified ionospheric regional model for telecommunication applications, *Radio Sci (USA)*, 28 (4) (1993) pp 603-612.

15 Holt J M & Zhang S R, A local empirical model of the E and F region ionosphere based on 30 years of Millstone Hill incoherent scatter data, *AGU Fall Meeting (USA)*, (2002) SA21A-0425.

16 McKinnel L A & Poole A W V, A neutral network based electron density model for the E-layer, *Adv Space Res (UK)*, 31 (3) (2003) pp 586-595.

17 Bilitza D, International Reference Ionosphere 2000, *Radio Sci (USA)*, 36 (2) (2001) pp 261-275.

18 Adeniyi J O, Oladipo O A & Radicella S M, Variability of foF2 for an equatorial station and comparison with foF2 maps in IRI model, *J Atmos Sol-Terr Phys (UK)*, 69 (2007) pp 721-733.

19 Ehinlafa O E & Adeniyi J O, Comparison of observed hmF2 and IRI 2007 model with M(300) F2 estimation of hmF2 during high solar activity for an equatorial station, *Indian J Radio Space Phys*, 42 (2013) pp 82-88.

20 Bilitza D, Obrou O K, Adeniyi J O & Oladipo, Variability of foF2 in the equatorial ionosphere, *Adv Space Res (UK)*, 34 (2004) pp 1901-1906.

21 Akala A O, Somoye E O, Adeloye A B & Rabiu A B, Ionospheric foF2 variability at equatorial and low latitudes during high, moderate and low solar activity, *Indian J Radio Space Phys*, 40 (2011) pp 124-129.

22 Kouris S S & Muggleton L M, Diurnal variation in the E- layer ionization, *J Atmos Sol-Terr Phys (UK)*, 35(1973a) pp 133-139.

23 Araujo Pradere E A, Lois Menendez L & Durand Manterola H J, Morphological characteristics of ionospheric E layer over E1 Cerrillo, Mexico during magnetically quiet conditions, *Geofis Int (Mexxico)*, 35 (1) (1995) pp 77-81.